**YMTHE, Volume *30***

## Supplemental Information

# A chemokine regulatory loop induces cholesterol synthesis in lung-colonizing triple-negative breast cancer cells to fuel metastatic growth

**Bingchen Han, Felix Alonso-Valenteen, Zhe Wang, Nan Deng, Tian-Yu Lee, Bowen Gao, Ying Zhang, Yali Xu, Xinfeng Zhang, Sandrine Billet, Xuemo Fan, Stephen Shiao, Neil Bhowmick, Lali Medina-Kauwe, Armando Giuliano, and Xiaojiang Cui**

# Supplementary Materials for

## A Lung Fibroblast-mediated Chemokine-loop Induces Cholesterol Synthesis in Lung-colonizing Triple-negative Breast Cancer Cells to Drive Metastatic Growth

Bingchen Han, Felix Alonso-Valenteen, Zhe Wang, Nan Deng, Tian-Yu Lee, Bowen Gao, Ying Zhang, Yali Xu, Xinfeng Zhang, Sandrine Billet, Xuemo Fan, Stephen Shiao, Neil Bhowmick, Lali Medina-Kauwe, Armando Giuliano, Xiaojiang Cui

Correspondence to: Xiaojiang.cui@cshs.org and Bingchen.han@cshs.org

**This PDF file includes:**

**Figure. S1.**

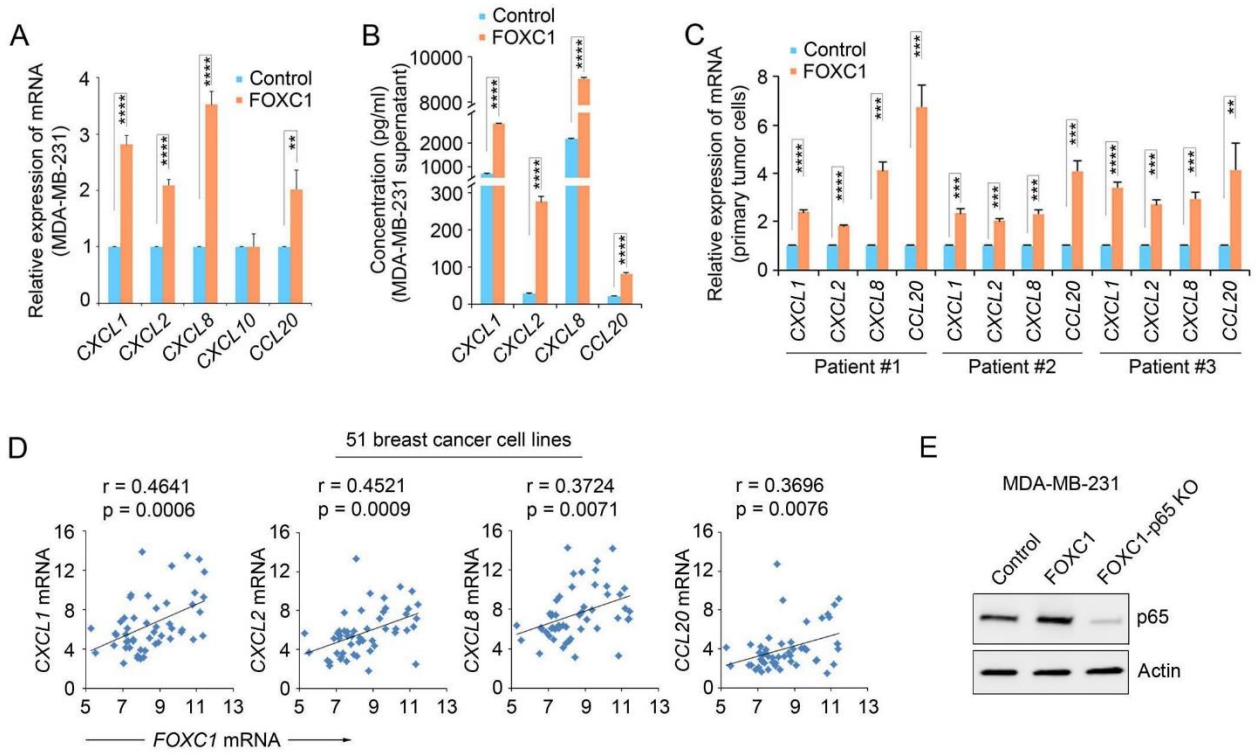


**Figure S1.** Chemokines CXCL1/2/8 and CCL20 are upregulated in TNBC.

**A,** real-time RT-PCR analysis of *CXCL1/2/8/10*, and *CCL20* in control and FOXC1-overexpressing MDA-MB-231 cells. **B,** ELISA of the CXCL1/2/8, and CCL20 levels in the supernatant of control and FOXC1-overexpressing MDA-MB-231 cells. **C,** real-time RT-PCR analysis of *CXCL1/2/8*, and *CCL20* in primary tumor cells of three TNBC patients. **D,** Pearson correlation analysis between *FOXC1* and *CXCL1/2/8*, or *CCL20* mRNA levels in 51 human breast cancer cell lines (include luminal A, luminal B, HER2-enriched, basal-like, and normal-like molecular subtypes). **E,** western blotting of p65 protein in p65 wildtype and p65 KO MDA-MB-231 cells. Actin was used as control. The bar graph indicates mean ± SD (n = 3). ** p<0.01, *** p<0.001, **** p<0.0001.

**Figure. S2.**

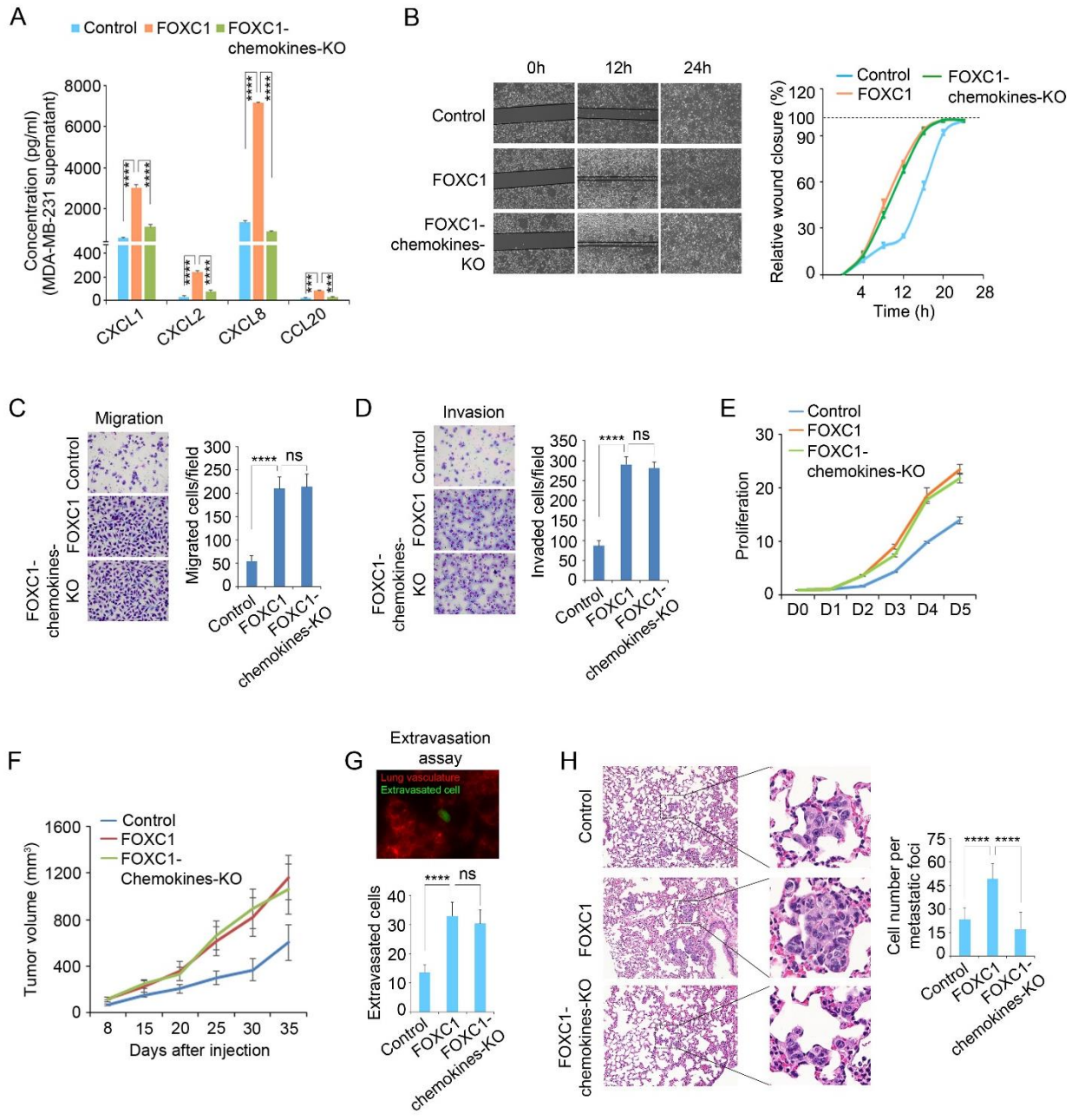


**Figure S2.** CXCL1/2/8 promote lung metastasis of TNBC cells.

**A,** ELISA analysis of the CXCL1/2/8 and CCL20 levels in the supernatant of different MDA-MB-231 sublines. **B-E,** wound healing (**B**), migration (**C**), invasion (**D**), and proliferation (**E**) assays of different MDA-MB-231 sublines. **F,** orthotopic xenograft models to evaluate the growth

capacities of different MDA-MB-231 mammary tumors. **G,** extravasation assays of different MDA-MB-231 sublines injected via mouse tail vein. Representative image shows the migrated cancer cell and the lung vasculature, which were labeled by CellTracker Green CMFDA and rhodamine-lectin, respectively. Magnification, 400×. The bar graph indicates mean ± SD (n = 5 slides). **H,** outgrowth of different MDA-MB-231 sublines in lung tissue. $0.5\times10^6$ cells were injected into mice through the tail vein. Lungs were collected 5 days after injection and sectioned followed by hematoxylin-eosin (HE) staining. Cell numbers of each metastatic foci were counted. The bar graph indicates mean ± SD (n = 10 foci. Two representative images were analyzed from each mouse, five mice were examined). ***, $p<0.001$, ****, $p<0.0001$.

**Figure. S3.**

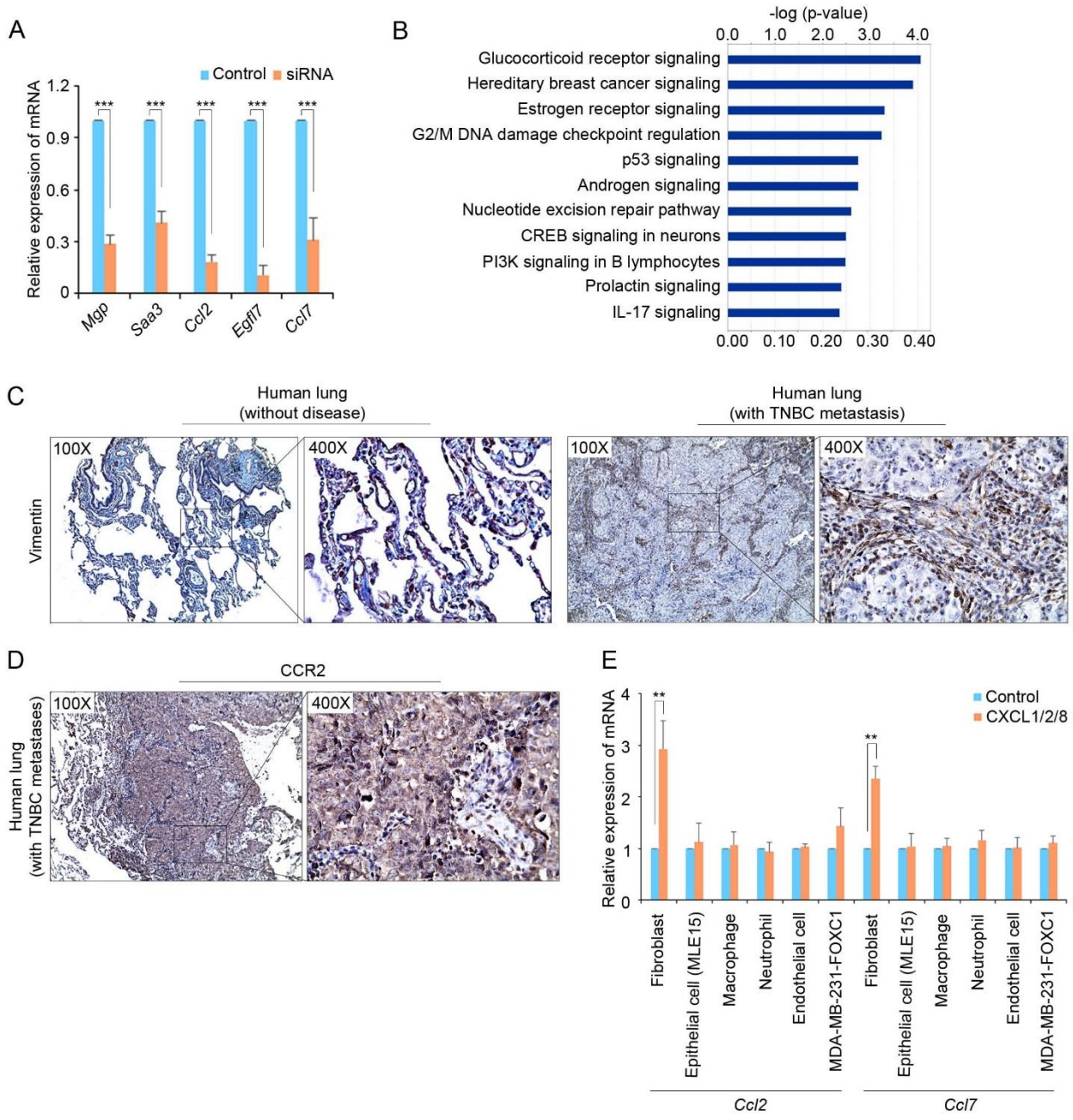


**Figure S3.** Lung fibroblasts increase CCL2/7 expression during TNBC lung metastasis formation. **A,** real-time RT-PCR assays to confirm the siRNA-mediated knockdown of different genes in isolated mouse lung fibroblasts. **B,** gene ontology (GO) analysis of the upregulated genes. RNA-

Seq experiments were performed in control and recombinant human CXCL1(8 nM)/2(2 nM)/8(20 nM) proteins-treated mouse lung fibroblasts. **C,** immunohistochemistry (IHC) staining of Vimentin in normal human lungs and lungs with TNBC metastases. **D,** IHC assay of CCR2 staining in human lungs with TNBC metastases. **E,** real-time RT-PCR assays of *Ccl2/7* mRNAs expression in lung fibroblasts, immortalized mouse lung epithelial cells (MLE15), macrophages, neutrophils, endothelial cells, and MDA-MB-231-FOXC1 cells. The bar graph indicates mean ± SD (n = 3). ** $p<0.01$, ***, $p<0.001$.

**Figure. S4.**

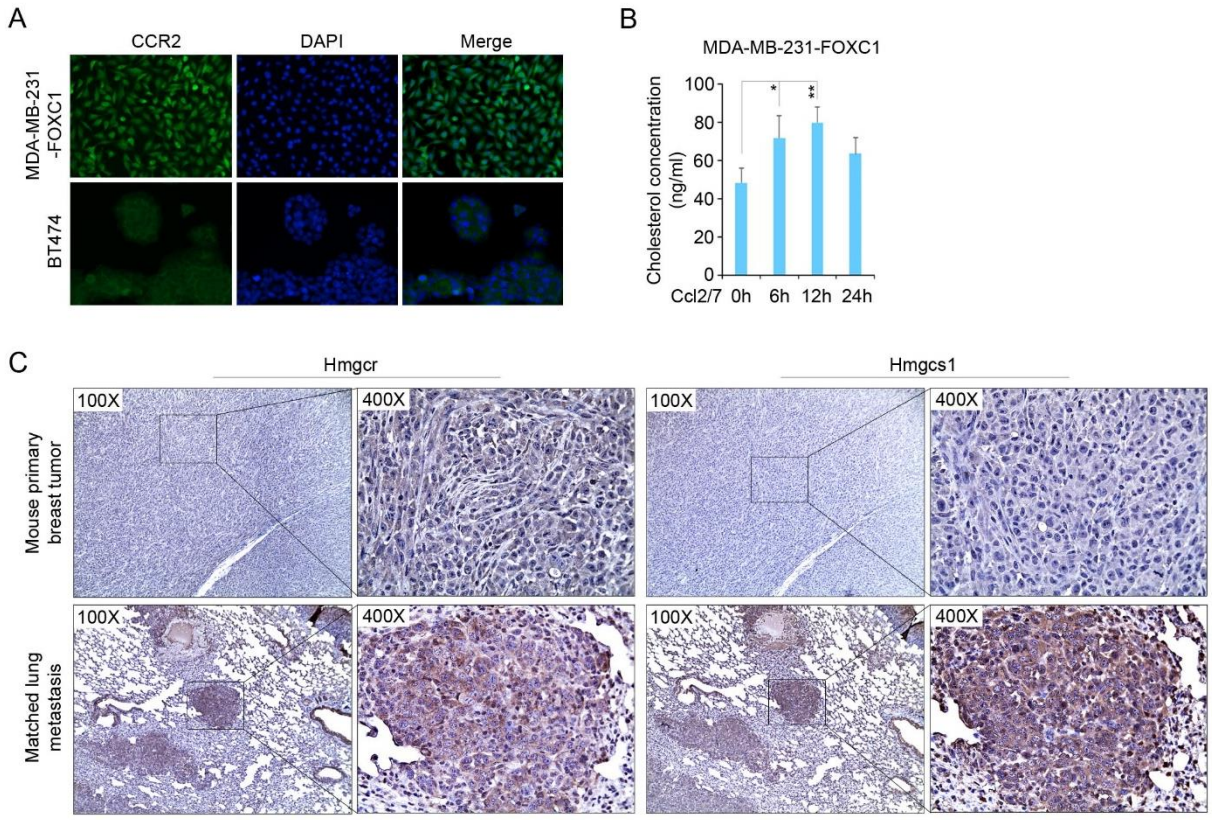


**Figure S4.** Lung fibroblast-derived CCL2/7 stimulate cholesterol synthesis in the lung-colonizing TNBC cells.

**A,** immunofluorescence staining of CCR2 in FOXC1-overexpressing MDA-MB-231 cells. BT474 cells expressing lower level of CCR2 were used as a control. Magnification, 200×. **B,** ELISAs of cholesterol concentrations in the supernatant of mouse Ccl2(10 nM)/7(50 nM)-treated FOXC1-overexpressing MDA-MB-231 cells at different timepoints. **C,** IHC of Hmgcr and Hmgcs1 in mouse 4T1 primary breast tumors and matched lung metastases. The bar graph indicates mean ± SD (n = 3). * $p<0.05$, ** $p<0.01$.

**Figure. S5.**

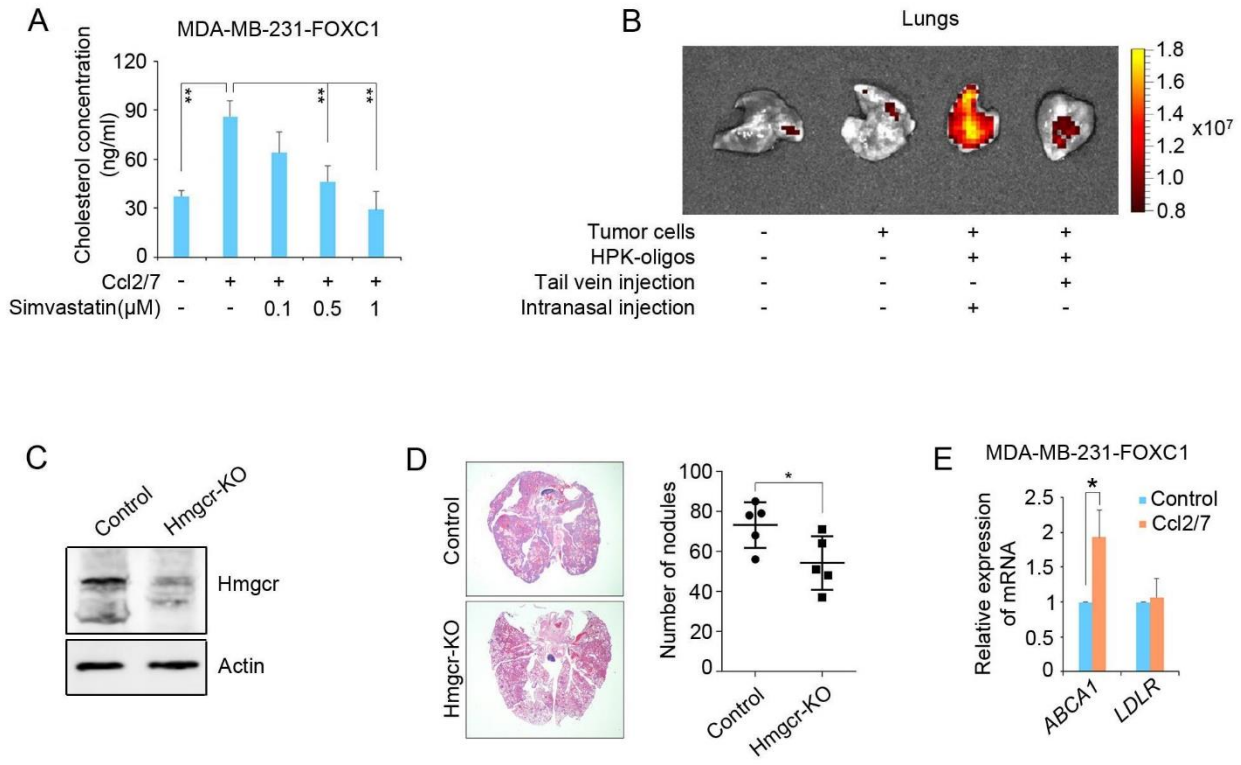


**Figure S5.** Targeting cholesterol synthesis in lung-colonizing TNBC cells to inhibit lung metastasis formation.

**A,** ELISA of cholesterol concentrations in the supernatant of FOXC1-overexpressing MDA-MB-231 cells treated with simvastatin. **B,** evaluation of the targeted delivery of nanoparticle HPK to mouse lung tissue. $0.5\times10^6$ 4T1 cells were injected into BALB/c wild-type mice through the tail vein. After 48 hours, 1.5μg HPK-oligo (Alexa Fluor 680-conjugated) were administered into mice intranasally or through the tail vein. Mouse lungs were collected 3 hours after the delivery and scanned by the IVIS Lumina XR *in vivo* imaging system. **C,** western blotting to confirm Hmgcr knockout in 4T1 cells. Actin was used as control. **D,** syngeneic mouse models to evaluate lung metastasis formation capacity. $0.5\times10^6$ control or Hmgcr-KO 4T1 cells were injected into mice through the tail vein (n = 5). Mouse lungs were collected 2 weeks after the injections. Metastatic

nodules were counted (right panel) and lung sections were stained by HE (left panel). E, real-time RT-PCR analysis of *ABCA1* and *LDLR* in Ccl2/7-treated MDA-MB-231-FOXC1 cells. The bar graph indicates mean ± SD (n = 3). *, $p<0.05$. **, $p<0.01$.

**Table S1.** Positive correlation between FOXC1 and chemokines in various breast tumor gene expression datasets.

| | CXCL1 | | CXCL2 | | CXCL8 | | CCL20 | | | | |
|---|---|---|---|---|---|---|---|---|---|---|---|
| Accession number | r-value | p-value | r-value | p-value | r-value | p-value | r-value | p-value | Sample size | Publication | PMID |
| GSE21653 | 0.447 | 1.80E-14 | 0.387 | 5.90E-11 | 0.342 | 9.80E-09 | 0.437 | 8.40E-14 | 266 | Sabatier et al., 2011 | 20490655 |
| GSE3494 | 0.458 | 2.20E-14 | 0.338 | 4.10E-08 | 0.269 | 1.50E-05 | 0.29 | 3.00E-06 | 251 | Miller et al., 2005 | 16141321 |
| GSE2034 | 0.397 | 3.10E-12 | 0.353 | 7.80E-10 | 0.247 | 2.30E-05 | 0.381 | 2.70E-11 | 286 | Wang et al., 2005 | 15721472 |
| GSE12276 | 0.438 | 5.70E-11 | 0.399 | 3.40E-09 | 0.2 | 4.10E-03 | 0.43 | 1.40E-10 | 204 | Bos et al., 2009 | 19421193 |
| GSE25066 | 0.283 | 8.20E-11 | 0.291 | 2.10E-11 | 0.232 | 1.30E-07 | 0.267 | 9.40E-10 | 508 | Hatzis et al., 2011 | 21558518 |
| GSE36771 | 0.559 | 3.90E-10 | 0.373 | 7.50E-05 | 0.401 | 1.90E-05 | 0.374 | 7.20E-05 | 107 | Caldon et al., 2012 | 22564725 |
| GSE2109 | 0.253 | 1.60E-06 | 0.199 | 1.80E-04 | 0.227 | 1.80E-05 | 0.232 | 1.10E-05 | 351 | EXPO | |
| GSE1456 | 0.36 | 3.20E-06 | 0.248 | 1.60E-03 | 0.15 | 0.06 | 0.239 | 2.40E-03 | 159 | Pawitan et al., 2005 | 16280042 |
| GSE28844 | 0.468 | 1.40E-04 | 0.564 | 2.20E-06 | 0.34 | 7.40E-03 | 0.24 | 0.06 | 61 | Vera-Ramirez et al., 2013 | 23326553 |
| GSE7390 | 0.256 | 2.70E-04 | 0.313 | 7.10E-06 | 0.168 | 0.02 | 0.247 | 4.40E-04 | 198 | Desmedt et al., 2007 | 17545524 |
| GSE5462 | 0.327 | 3.40E-04 | 0.431 | 1.30E-06 | 0.284 | 2.00E-03 | 0.298 | 1.20E-03 | 116 | Miller et al., 2007 | 17885619 |
| GSE2603 | 0.327 | 1.10E-03 | 0.205 | 0.04 | 0.37 | 2.00E-04 | 0.302 | 2.80E-03 | 96 | Minn et al., 2005 | 16049480 |
| GSE42568 | 0.292 | 1.10E-03 | 0.263 | 3.60E-03 | 0.186 | 0.04 | 0.222 | 0.01 | 121 | Clarke et al., 2013 | 23740839 |
| GSE5460 | 0.264 | 3.20E-03 | 0.143 | 0.11 | 0.252 | 5.00E-03 | 0.352 | 6.50E-05 | 123 | Lu et al., 2008 | 18297396 |

Regression analysis was performed for the statistical analysis.

**Table S2.** The sequences of guide RNAs used in CRISPR-dCas9 knockout experiments.

| *Gene name* | *Number* | *Guide RNA (gRNA) sequence* | *Accession number* |
|---|---|---|---|
| Human *CXCL1* | #1 | TCATCGAAAAGATGCTGAAC | NM_001511.3 |
| | #2 | GGAGCAGCAGTGCCACTCGC | |
| | #3 | GCCGCTGGCCGGCGCGCAGC | |
| Human *CXCL2* | #1 | CGCAGGAGCCGGGGATTGCT | NM_002089.3 |
| | #2 | CGCGCCGGCTGGCGGCCACC | |
| | #3 | CAAGAACATCCAAAGTGTGA | |
| Human *CXCL8* | #1 | CTAAGTTCTTTAGCACTCCT | NM_000584.3 |
| | #2 | TGTAAACATGACTTCCAAGC | |
| | #3 | GAACTGAGAGTGATTGAGAG | |
| Human *CCL20* | #1 | TACCTTCTGATTCGCCGCAG | NM_004591.2 |
| | #2 | AATATATTGTGCGTCTCCTC | |
| | #3 | CAAACTCTTGGTACAGCACA | |
| Human *p65* | #1 | GCTTCCGCTACAAGTGCGAG | NM_021975.3 |
| | #2 | AGCGCCCCTCGCACTTGTAG | |
| | #3 | CAAGTGCGAGGGGCGCTCCG | |
| Mouse *Hmgcr* | #1 | CCGGATGCATGGCCTCTTCG | NM_008255.2 |
| | #2 | TCAAGACTTTTCCGGATGCA | |
| | #3 | CCACGAAGAGGCCATGCATC | |

**Table S3.** The primers used in the real-time PCR assays.

| *Gene name* | *Sequence* | | *Accession number* |
|---|---|---|---|
| Human *CXCL1* | Forward | AGGCAGGGGAATGTATGTGC | NM_001511.3 |
| | Reverse | AGCCCCTTTGTTCTAAGCCA | |
| Human *CXCL2* | Forward | AGATCAATGTGACGGCAGGG | NM_002089.3 |
| | Reverse | TCTCTGCTCTAACACAGAGGGA | |
| Human *CXCL8* | Forward | GGTGCAGTTTTGCCAAGGAG | NM_000584.3 |
| | Reverse | TTCCTTGGGGTCCAGACAGA | |
| Human *CXCL10* | Forward | ATATGGCACACTAGCCCCAC | NM_001565.3 |
| | Reverse | ATGCTGATGCAGGTACAGCG | |
| Human *CCL20* | Forward | TGTCAGTGCTGCTACTCCAC | NM_004591.2 |
| | Reverse | ATTTGCGCACACAGACAACT | |
| Human *CCL2* | Forward | ACCTGGACAAGCAAACCCAA | NM_002982.3 |
| | Reverse | AGGGTGTCTGGGGAAAGCTA | |
| Human *CCL7* | Forward | GAGATCTGTGCTGACCCCAC | NM_006273.3 |
| | Reverse | CCACTCTGAGAAAGGACAGGG | |
| Human *HMGCS1* | Forward | GTCACGCTTGTGCCCGAA | NM_001098272.2 |
| | Reverse | CTGGCCCAAGCCAATGGTAT | |
| Human *MSMO1* | Forward | TTCCGAGGTTGGAACACCTGG | NM_006745.4 |
| | Reverse | TGCAGAGGATTCTCAGGTAAAAGT | |
| Human *SC5D* | Forward | GCTAGGACAGTTTGCAGAGC | NM_006918.4 |
| | Reverse | TAGCTCAGTGTTGCACAGAAGA | |
| Human *SQLE* | Forward | CGTGCTGGTGTTCCTCTCG | NM_003129.3 |
| | Reverse | TTGGTTCCTTTTCTGCGCCTC | |
| Human *IDI1* | Forward | GGGACCGGCGGTTGTC | NM_004508.2 |
| | Reverse | AAAGCTCGATGCAATAATCCTTTC | |
| Human *CYP51A1* | Forward | GACCTCGGCCTTCAGTGTTT | NM_000786.3 |
| | Reverse | GGAGGACTTTTCACCCCTGC | |
| Human *NSDHL* | Forward | CGCCTACGGACGGAAAAGAAA | NM_015922.2 |
| | Reverse | CACTGTGCATCTCTTGGCCT | |
| Human *DHCR7* | Forward | AAGCGAGGCCAGGGGAA | NM_001360.2 |
| | Reverse | TGGCTTTGGGAATGTTGGGT | |
| Human *HSD17B7* | Forward | TCATCTCGCAGTGCAAGGAA | NM_016371.2 |
| | Reverse | GAGACCCTGCTGGTTGAAGT | |
| Human *HMGCR* | Forward | TCTTATTGGTCGAAGGCTCGT | NM_000859.2 |
| | Reverse | TCTCACTAGAGGCCACCGAA | |
| Human *MVD* | Forward | ATCAAGTACTGGGGCAAGCG | NM_002461.1 |
| | Reverse | CAAATCCGGTCCTCGGTGAA | |
| Human *FDFT1* | Forward | AAGGGGCAGTGAAGATTCGG | NM_004462.3 |
| | Reverse | AACGACAGGTAGATGGGGGA | |
| Human *MVK* | Forward | TTCCCAGGAGCCATGTTGTC | NM_000431.2 |
| | Reverse | TGGGTAAGCTGAGGTCCACT | |
| Human *ABCA1* | Forward | GCTCTCAGACCTGGGCATTT | NM_005502.4 |
| | Reverse | CCTTTGCCATCCATCCCACT | |

| | | | |
|---|---|---|---|
| Human *LDLR* | Forward | CAGCTACCCCTCGAGACAGA | NM_000527.5 |
| | Reverse | CACTGTCCGAAGCCTGTTCT | |
| Human *GAPDH* | Forward | ATGGGTGTGAACCATGAGAA | NM_002046.4 |
| | Reverse | GTGCTAAGCAGTTGGTGGTG | |
| Mouse *Mgp* | Forward | GGCGAGCTAAAGCCCAAAAG | NM_008597.3 |
| | Reverse | AAGTAGCGGTTGTAGGCAGC | |
| Mouse *Saa3* | Forward | AGCCAAAGATGGGTCCAGTT | NM_011315.3 |
| | Reverse | ATAGTTCCCCCGAGCATGGA | |
| Mouse *Ccl2* | Forward | CAGGTCCCTGTCATGCTTCT | NM_011333.3 |
| | Reverse | CCCATTCCTTCTTGGGGTCA | |
| Mouse *Egfl7* | Forward | AGTTCAGTGGTGAGGGGTCC | NM_178444.4 |
| | Reverse | TGGTCTGCATCTGTAAGTGGG | |
| Mouse *Ccl7* | Forward | GATCTCTGCCACGCTTCTGT | NM_013654.3 |
| | Reverse | ATAGCCTCCTCGACCCACTT | |
| Mouse *Gapdh* | Forward | TGTGAACGGATTTGGCCGTA | BC096042.1 |
| | Reverse | AGATGCCTGCTTCCCATTCT | |